

## PDF hosted at the Radboud Repository of the Radboud University Nijmegen

The following full text is a publisher's version.

For additional information about this publication click this link.

<http://hdl.handle.net/2066/29592>

Please be advised that this information was generated on 2017-12-05 and may be subject to change.

## Macroscopic Size Effects in Second Harmonic Generation from Si(111) Coated by Thin Oxide Films: The Role of Optical Casimir Nonlocality

O. A. Aktsipetrov,<sup>1,\*</sup> A. A. Fedyanin,<sup>1</sup> E. D. Mishina,<sup>1</sup> A. A. Nikulin,<sup>1</sup> A. N. Rubtsov,<sup>1</sup>

C. W. van Hasselt,<sup>2</sup> M. A. C. Devillers,<sup>2</sup> and Th. Rasing<sup>2</sup>

<sup>1</sup>*Department of Physics, Moscow State University, Moscow 119899, Russia*

<sup>2</sup>*Research Institute for Materials, University of Nijmegen, Toernooiveld 1, NL 6525 ED Nijmegen, The Netherlands*

(Received 27 March 1996)

Optical second harmonic generation from Si(111)-SiO<sub>2</sub> interface shows a strong nonmonotonic dependence on the oxide thickness between 2 and 300 nm. The Brewster angle of incidence, *p*-in, *p*-out combination of polarizations and strong, uniform suppression of this effect by near-index matching fluid exclude trivial multiple reflections and microscopic interface effects. The observation can be interpreted to originate from the optical (Casimir) nonlocality stemming from the thickness-dependent electron-electron interaction via virtual photons of the quantized electromagnetic field. [S0031-9007(96)01932-1]

PACS numbers: 42.65.Ky, 03.70.+k, 78.20.-e

Zero-point fluctuations of the electromagnetic field give rise to long-range (Casimir) interactions, that, for example, in the nonretarded limit are responsible for the van der Waals force [1]. Recent high precision measurements of the forces between an atom and a metallic [2] or dielectric [3] surface has renewed the interest in these fluctuation phenomena [4]. However, Casimir effects may have much wider consequences, ranging from biology to cosmology (see [5] and [6]). A beautiful maritime analogy of the Casimir effect was recently discussed in [7], whereas vacuum fluctuations of the gravitational field may set a limit for the accuracy of length measurements [8]. Generally, retardation effects start playing a role when the time necessary for the exchange of information (e.g., the travel time of a photon), exceeds a characteristic fluctuation time of the system of interest. Therefore, the relevant length scale that plays a role is  $c/2\omega_0$ , with  $c$  is the speed of light and  $\omega_0$  is the typical fluctuation frequency. The Casimir effects will manifest themselves when there are some sort of restrictions for the fluctuation spectrum, i.e., the boundary conditions imposed by a cavity. We will show that the oxide layer of a Si-SiO<sub>2</sub> structure can be responsible for nonlocal effects in its nonlinear optical response that stem from the Casimir interaction.

Based on the inversion symmetry breaking at an interface, optical second harmonic generation (SHG) at surfaces and interfaces of centrosymmetric media has been perceived as an extremely sensitive and versatile probe for surface-science studies [9], in particular, for a buried interface like Si-SiO<sub>2</sub>. The inversion symmetry breaking at the Si-SiO<sub>2</sub> interface has been associated with a crystalline structure discontinuity [10], disordering [11], local strain [12], or band bending [13,14].

Typically the spatial scale characterizing a size effect observed in an SHG experiment is an informative "fingerprint" of its underlying mechanism. Two specific length scales can be distinguished for the oxide-thickness dependence of SHG from Si(111)-SiO<sub>2</sub>: (i)  $r_0 \sim 1$  nm, deter-

mined by the morphological and electronic structure of the interface [12,15], and a measure of the microscopic optical nonlocality [16], and (ii)  $l_{\text{opt}} \sim 100$  nm determining the nonuniformity of the optical fields in the medium due to optical interference [17]. In these two limiting cases the macroscopic and microscopic aspects of the problem separate quite distinctly and can be treated theoretically using traditional approaches.

The scale  $r_0$  enters into the quantum-mechanical expression for the interface quadratic optical susceptibility. In the electric-dipole approximation the quadratic response of a system to a monochromatic external field  $\mathbf{E}^{\text{ext}}(\mathbf{r}, t)$  is calculated using the Hamiltonian  $H - \int \mathbf{P}(\mathbf{r})\mathbf{E}^{\text{ext}}(\mathbf{r}, t) d^3r$ , where  $H$  is the Hamiltonian of the system and the operator of the macroscopic polarization  $\mathbf{P}(\mathbf{r})$  is obtained by spatial averaging the microscopic dipole-moment density over the volume  $\sim r_0^3$ . A conventional approximation for  $H$  (denoted by  $H_0$ ) includes the interaction of the charged particles of the medium with the modes of the electromagnetic field with wavelengths of the order of the lattice constant, whereas the interaction with longer-wavelength modes is neglected [16]. This yields the local quadratic susceptibility  $\chi^{\text{bare}}$  vanishing everywhere except in a layer of thickness  $\sim r_0$  at the Si-SiO<sub>2</sub> interface, where the inversion symmetry is broken. The scale  $l_{\text{opt}}$  characterizing the linear-optical features of the inhomogeneous medium appears in the solution of the macroscopic Maxwell equations, and may lead to a very strong SHG thickness dependence, as observed experimentally [17].

However, for a typical optical mode  $\hbar\omega_0 = 3$  eV, the relevant length scale for retardation effects  $c/2\omega_0 \approx l_{\text{opt}}$ . This means that also less trivial size effects may occur within the intermediate range  $r_0 \leq D \leq l_{\text{opt}}$  as a result of size dependent nonlocal optical effects.

In this paper we show that this so-called optical Casimir nonlocality can give rise to a substantial SHG thickness dependence from Si-SiO<sub>2</sub> interfaces, for oxide thicknesses in the range of 2–300 nm. The interface localization of

the nonlinear optical source and the possibility to vary its inhomogeneous environment (i.e., the oxide thickness) systematically appear to be essential ingredients for the observability of these nonlocal optical effects. The experiments have been carefully designed to allow an unambiguous interpretation of the data: (i) the sample preparation technique is chosen in such a way to provide a uniform “sampling” of the whole SiO<sub>2</sub>-layer thickness range  $r_0 \leq D \leq l_{\text{opt}}$  without affecting the buried Si(111)-SiO<sub>2</sub> interface at the microscopic level; (ii) to avoid the effects of multiple reflections the SHG measurements are carried out for the *p*-in, *p*-out polarization combination at Brewster angle of incidence on the outer (SiO<sub>2</sub>-air) interface; (iii) to reveal the role of the SiO<sub>2</sub>-air interface the SHG measurements in air are complemented by those for the samples immersed in a (almost) refractive-index-matching liquid.

The samples used were *p*-type (2–5 Ω cm) Si(111) ( $\pm 0.5^\circ$ ) wafers on which a high quality thermal oxide with a thickness of 300 nm was grown previously at 1000 °C in a dry oxygen ambient environment. The wafers were annealed at a slightly higher temperature in a N<sub>2</sub> atmosphere to fabricate a smooth Si-SiO<sub>2</sub> interface. The wafers oxidized from the same batch were etched with a buffered NH<sub>4</sub>F solution with the rate of  $\sim 25$  nm/min in  $3 \times 3$  and  $5 \times 5$  checkerboard configurations to produce samples with the oxide thickness ranging in a steplike manner from 2 to 300 nm.

Single-wavelength ellipsometry with a HeNe laser (632.8 nm) was used to measure the oxide layer thicknesses prior to and after etching and to check the thickness uniformity for each particular square on the checkerboard samples. High resolution transmission electron microscopy images were made for both unetched and etched wafers in order to verify that the originally smooth Si-SiO<sub>2</sub> interface, with a corrugation of just a few atomic

layers over macroscopic distances of  $\sim 100$  μm along the interface remained so after etching.

For the SHG experiments the output at 1064 nm of a *Q*-switched Nd:YAG laser was used, with 10 ns pulses of 10–15 mJ in a 5 mm diameter spot, well below the damage threshold. The SHG signal was recorded using standard gated electronics. The SHG measurements were performed for the *p*-in, *p*-out combination of polarizations, at an angle of incidence on the SiO<sub>2</sub>-air interface of 55.5°, which is very close to the Brewster angles for the fundamental and SHG radiation (55.3° and 55.7°, respectively).

The SHG intensity  $I_{2\omega}^{p,p}$  as a function of the azimuthal angle for oxide thicknesses of 34 and 65 nm is shown in the inset of Fig. 1. This dependence can be described in the following form:

$$I_{2\omega}^{p,p}(D, \varphi) = |A(D) + B(D)e^{i\psi(D)} \cos 3\varphi|^2, \quad (1)$$

where  $A(D)$  and  $B(D)$  are the real thickness-dependent amplitudes of the isotropic and anisotropic components of the quadratic polarization, respectively, and  $\psi(D)$  is the relative phase shift between them. The plots for  $A$ ,  $B$ , and  $\psi$  versus  $D$  for the experiments in air and water are shown in Fig. 1. A very pronounced  $D$  dependence of all three quantities occurs for the samples in air. It is noteworthy that (i) the scale of the initial steep rise in  $A(D)$ ,  $B(D)$ , and  $\psi(D)$  is about 50–100 nm; (ii) in the thickness dependence of  $A$ ,  $B$ , and  $\psi$  there are distinct oscillations within the range from 100 to 300 nm. A strong suppression of all these SHG thickness dependences is observed for the samples being immersed in water.

At first, this last observation suggests a trivial optical interference effect that is suppressed by the near index matching properties of the water ( $n_{\text{H}_2\text{O}} = 1.33$ ,

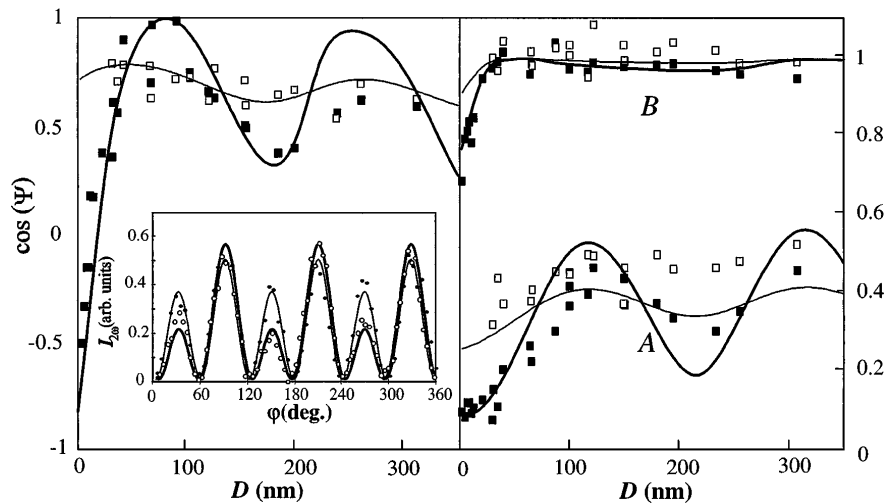


FIG. 1. The isotropic and anisotropic SHG components  $A$  and  $B$  and the cosine of the relative phase shift  $\psi$  vs oxide thickness  $D$ . Squares, experiment; lines, theory (■, thick lines: sample in air; □, thin lines: sample in water). The inset shows the rotational SHG anisotropy for  $D = 34$  nm (●, thin line) and  $D = 65$  nm (○, thick line).

$n_{\text{SiO}_2} = 1.45$ ). However, this is excluded by the Brewster angle geometry. Alternative standard explanations for the oxide-thickness dependence can also be excluded. The band bending by the charge trapped in the oxide layer [14] or the strain of the subsurface Si layer [12], in principle, can be thickness dependent; yet the suppression of their thickness dependence by immersion cannot be as uniform as we observed within the whole oxide-thickness range from 2 to 300 nm. The contribution to SHG from the crystalline  $\text{SiO}_2$  transition layer [11] is thickness independent for  $D \geq 10$  nm; moreover, immersion cannot affect this nonlinearity. The interference between two nonlinear sources situated at the Si-SiO<sub>2</sub> and SiO<sub>2</sub>-air interfaces can exist at the Brewster angle of incidence and be suppressed upon immersion; however, the contrast of the corresponding interference pattern is too low because the SiO<sub>2</sub>-air interface nonlinearity is by at least 2 orders of magnitude smaller than that of the Si(111)-SiO<sub>2</sub> interface [18].

The key idea of our interpretation of the experimental results is that the size effect is related to a long-range optical nonlocality stemming from the interaction of the three-layer medium (Si-SiO<sub>2</sub>-air) with the optical-range eigenmodes of the quantized electromagnetic field (QEF). To proceed with this hypothesis in a way known from the theory of the Casimir force [1] we consider the Hamiltonian that explicitly includes the interaction of electrons with the optical QEF modes,

$$H = H_0 + W + \sum_{\Lambda} \hbar \omega_{\Lambda} a_{\Lambda}^{\dagger} a_{\Lambda}, \quad (2)$$

where  $a_{\Lambda}^{\dagger}$  and  $a_{\Lambda}$  are photon creation and annihilation operators for an optical eigenmode  $\Lambda$  with frequency  $\omega_{\Lambda}$ ;  $W$  is the operator of the interaction between the quantized optical field and the electron subsystem

$$W = - \int \mathbf{P}(\mathbf{r}) \mathbf{E}(\mathbf{r}) d^3 r, \quad (3)$$

with the electric-field operator  $\mathbf{E}(\mathbf{r}) = \sum_{\Lambda} \mathbf{u}_{\Lambda}(\mathbf{r}) a_{\Lambda} + \text{H.c.}$  The function  $\mathbf{u}_{\Lambda}(\mathbf{r})$  describing the spatial behavior of  $\mathbf{E}(\mathbf{r})$  is the properly normalized solution of the classical electrodynamical problem for the three-layer system with bare (i.e., determined by  $H_0$ ) dielectric constants. The presence of the operator  $W$  in the Hamiltonian leads to an additional long-range electron-electron interaction, mediated by virtual optical-wavelength photons. This results in an interaction between the (electrical neutral) microscopic polarization sources of volume  $r_0^3$  via virtual QEF photons (see Fig. 2). This effect has the same nature as the Casimir force acting between macroscopic solids [19] and results in a drastic change in the quadratic response to the external optical field  $\mathbf{E}^{\text{ext}}(\mathbf{r}, t)$ . The corresponding second-order susceptibility  $\chi^{\text{dressed}}$  calculated in the dipole approximation is essentially nonlocal, in contrast

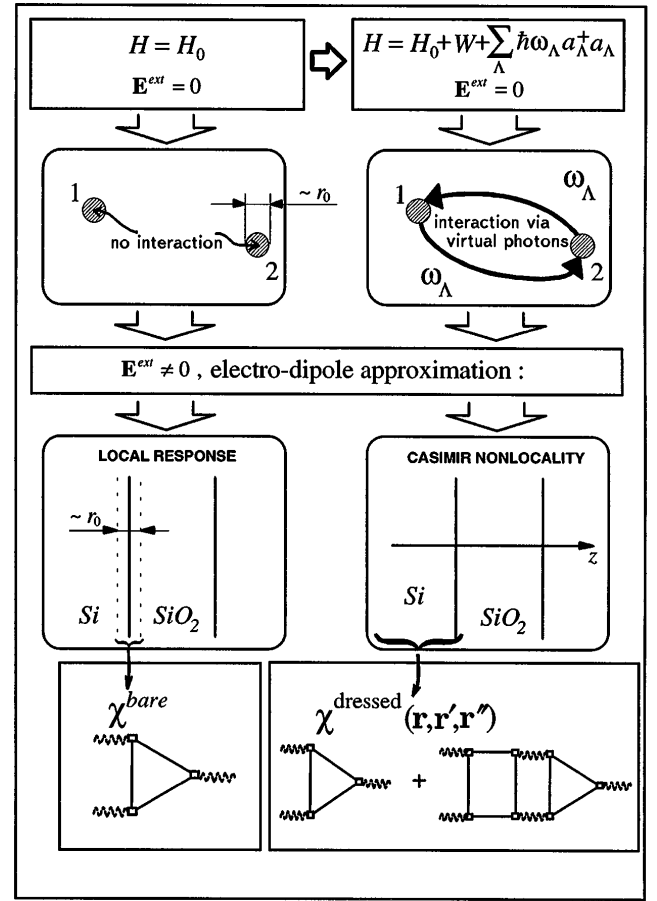


FIG. 2. Contributions to  $\chi^{(2)}$ . The left-hand side shows the sketch of the classical formalism to calculate  $\chi^{\text{bare}}$ . The right-hand side shows the sketch of the quantum electrodynamic approach for  $\chi^{\text{dressed}}$  of an inhomogeneous system, taking both the Coulomb and retarding parts of the interaction into account.

with the conventional local dipole susceptibility  $\chi^{\text{bare}}$  [16]. We call this type of large-scale spatial nonlocality the optical Casimir nonlocality.

The quadratic susceptibility  $\chi^{\text{dressed}}$  given by the Hamiltonian (2) can be calculated by treating  $W$  as a perturbation. The diagrams representing the higher-order terms of this expansion consist of several compact electron parts that are connected with virtual-photon propagator lines giving rise to the Casimir nonlocality. One of such nonlocal diagrams is shown in Fig. 2. Because of the symmetry selection rules for the dipole-moment matrix elements, the electron parts with an odd number of vertices vanish everywhere except within the Si-SiO<sub>2</sub> interface layer of thickness  $r_0$ . Electron parts with even vertex numbers take nonzero values in the bulk of both Si and SiO<sub>2</sub>.

Taking into account the lowest-order nonlocal term given by the diagram in Fig. 2 we obtain the following expression:

$$\chi_{ijk}^{\text{dressed}}(\mathbf{r}, \mathbf{r}', \mathbf{r}'', \omega) = \delta(\mathbf{r}, \mathbf{r}') \delta(\mathbf{r}, \mathbf{r}'') \chi_{ijk}^{\text{bare}}(\mathbf{r}, \omega) + \delta(\mathbf{r}, \mathbf{r}'') \times \int_{-\infty}^{+\infty} X_{jlm}(\mathbf{r}', \omega, \Omega) Y_{npik}(\mathbf{r}, \omega, \Omega) \Gamma_{ln}(\mathbf{r}, \mathbf{r}', \Omega; D) \Gamma_{mp}(\mathbf{r}, \mathbf{r}', \omega - \Omega; D) d\Omega, \quad (4)$$

where  $\Gamma$  denotes the retarded Green function of the electromagnetic field [19] calculated in zeroth order of  $W$  and depending on frequency and oxide-layer thickness;  $\omega$  is the fundamental field frequency,  $\delta$  is the Dirac delta function. For the sake of brevity, we omit the explicit expressions for the tensors  $X$  and  $Y$  corresponding to the triangle and tetragon electron parts of the diagram, respectively. Their structure is similar to that of the quadratic and cubic susceptibilities of the medium.  $\chi^{\text{bare}}(r)$  is the local ( $D$ -independent) susceptibility.

The essential source of the thickness dependence is the virtual-photon Green function  $\bar{\Gamma}$  entering into the expression for  $\chi^{\text{dressed}}$  and containing  $D$  as a parameter. In optical terms the thickness dependence can be interpreted as originating from the multibeam interference for a whole set of virtual eigenmodes in the oxide layer. This interference is not eliminated by our choice of Brewster angle geometry, as this only affects one particular wave vector. However, immersion in refractive-index matching fluid does suppress this interference. This directly follows from Eq. (4), since the Green function  $\bar{\Gamma}$  becomes thickness independent in that case. Therefore, the thickness dependence of the SHG signal disappears upon immersion though the nonlocal Casimir contribution is still present.

For comparison with experiment we used a simple model that, however, contains all qualitative features of the effect. In particular,  $X$  and  $Y$  are taken in the factorized form,  $X_{ijk}(\Omega) = X_{ijk}\mu(\Omega)$ ,  $Y_{ijkl}(\Omega) = \delta_{ij}\delta_{kl}\mu(\Omega)$ , where  $X_{ijk}$  reproduces the tensorial features of the quadratic susceptibility of the Si(111)-SiO<sub>2</sub> interface [20] and the spectral function  $\mu(\Omega)$  is taken as a single peak positioned at 3.3 eV, the dominant feature in the SHG spectrum from Si-SiO<sub>2</sub> [12]. The thus obtained numerical results are plotted in Fig. 1 and show a quite good agreement with the experiments within the whole available thickness range. It is worth noting that the thickness dependence is only partially suppressed by immersion because the refractive index matching in water is not perfect.

Apparently the Casimir nonlocality that, generally speaking, contributes to the linear-optical response of the medium as well leads to a much weaker thickness dependence in a linear-optical analog of our experiment. In fact, nonlocal corrections to the linear susceptibility are described by diagrams which do not contain surface-localized triangle parts, and, as a result, the thickness dependence is eroded by the additional integration over the volume of the bulk medium. For the same reason we have neglected the thickness dependence of the bulk quadrupole-allowed [9] quadratic susceptibility of silicon.

Summarizing, we have observed a pronounced oxide-thickness dependence in the SHG response from Si-SiO<sub>2</sub> interface that can be attributed to a new type of nonlocal spatial effect: the optical Casimir nonlocality. The latter provides the most pronounced size dependence for the even-order interface nonlinearities of centrosymmetric media and is an intrinsically many-particle effect stemming from the effective electron-electron interaction via

the optical-range modes of the quantized electromagnetic field.

We are pleased to acknowledge stimulating discussions with L. V. Keldysh, P. V. Elyutin, D. N. Klyshko, Yu. A. Il'inskii, and A. G. Mal'shukov. We would like to thank S. Bakker for preparation of the thick thermal oxide.

\*Corresponding author.

Electronic address: aktsip@astra.phys.msu.ru

- [1] H. B. G. Casimir and D. Polder, *Phys. Rev.* **73**, 360 (1948).
- [2] V. Sandoghdar, C. I. Sukenik, E. A. Hinds, and S. Haroche, *Phys. Rev. Lett.* **68**, 3432 (1992).
- [3] A. Landragin, J.-Y. Courtois, G. Labeyrie, N. Vansteenkiste, C. I. Westbrook, and A. Aspect, *Phys. Rev. Lett.* **77**, 1464 (1996).
- [4] Yu. S. Barash and V. L. Ginzburg, in *The Dielectric Function of Condensed Matter*, edited by L. V. Keldysh, D. A. Kirzhnits, and A. A. Maradudin (North-Holland, Amsterdam, 1989), p. 389.
- [5] L. Spruch, *Science* **272**, 1452 (1996).
- [6] V. M. Mostepanenko and N. N. T. Trunov, *Sov. Phys. Usp.* **31**, 965 (1988).
- [7] S. L. Boersma, *Am. J. Phys.* **64**, 539 (1996).
- [8] M. T. Jaekel and S. Reynaud, *Phys. Lett. A* **185**, 143 (1994).
- [9] T. F. Heinz, in *Nonlinear Surface Electromagnetic Phenomena*, edited by H.-E. Ponath and G. I. Stegeman (North-Holland, Amsterdam, 1991), p. 355; Y. R. Shen, *Nature (London)* **337**, 519 (1989).
- [10] H. W. K. Tom, T. F. Heinz, and Y. R. Shen, *Phys. Rev. Lett.* **51**, 1983 (1983); O. A. Aktsipetrov, I. M. Baranova, and Yu. A. Il'inskii, *Zh. Eksp. Teor. Fiz.* **91**, 287 (1986) [*Sov. Phys. JETP* **64**, 167 (1986)]; C. W. van Hasselt, M. A. Verheijen, and Th. Rasing, *Phys. Rev. B* **42**, 9263 (1990).
- [11] C. Meyer, G. Lupke, U. Emmerichs, F. Wolter, H. Kurz, C. H. Bjorkman, and G. Lucovsky, *Phys. Rev. Lett.* **74**, 3001 (1995).
- [12] W. Daum, H.-J. Krause, U. Reichel, and H. Ibach, *Phys. Rev. Lett.* **71**, 1234 (1993).
- [13] C. H. Lee, R. K. Chang, and N. Bloembergen, *Phys. Rev. Lett.* **18**, 167 (1967).
- [14] O. A. Aktsipetrov and E. D. Mishina, *Dokl. Akad. Nauk SSSR* **274**, 62 (1984) [*Sov. Phys. Dokl.* **29**, 37 (1984)]; P. R. Fischer, J. L. Daschbach, and G. L. Richmond, *Chem. Phys. Lett.* **218**, 200 (1994).
- [15] T. F. Heinz, M. M. Loy, and W. A. Thompson, *J. Vac. Sci. Technol. B* **3**, 1467 (1985).
- [16] Yu. A. Il'insky and L. V. Keldysh, *Electromagnetic Response of Material Media* (Plenum Press, New York and London, 1994).
- [17] C. W. van Hasselt, M. A. C. Devillers, Th. Rasing, and O. A. Aktsipetrov, *J. Opt. Soc. Am. B* **12**, 33 (1995).
- [18] P. Guyot-Sionnest and Y. R. Shen, *Phys. Rev. B* **35**, 4420 (1987).
- [19] E. M. Lifshitz and L. P. Pitaevsky, *Statistical Mechanics* (Nauka, Moscow, 1978), Pt. 2.
- [20] J. E. Sipe, D. J. Moss, and H. M. van Driel, *Phys. Rev. B* **35**, 1129 (1987).